

Ordered Phases and Quantum Criticality in Cubic Heavy Fermion Compounds

Silke Paschen

*Institute of Solid State Physics, Vienna University of Technology,
Wiedner Hauptstr. 8-10, 1040 Vienna, Austria*

Julio Larrea J.

*Institute of Solid State Physics, Vienna University of Technology,
Wiedner Hauptstr. 8-10, 1040 Vienna, Austria and
Physics Department, University of Johannesburg,
P.O. Box 524, Auckland Park 2006, South Africa*

(Dated: March 7, 2014)

Abstract

Quantum criticality in cubic heavy fermion compounds remains much less explored than in quasi-two-dimensional systems. However, such materials are needed to broadly test the recently suggested global phase diagram for heavy fermion quantum criticality. Thus, to boost these activities, we review the field, with focus on Ce-based systems with temperature–magnetic field or temperature–pressure phase diagrams that may host a quantum critical point. To date, CeIn_3 and $\text{Ce}_3\text{Pd}_{20}\text{Si}_6$ are the only two among these compounds where quantum critical behaviour has been systematically investigated. Interestingly, both show Fermi surface reconstructions as function of the magnetic field that may be understood in terms of Kondo destruction quantum criticality.

I. INTRODUCTION

Heavy fermion compounds are at the forefront of research in quantum criticality.^{1,2} The competition between the Kondo interaction that tends to screen local moments and the RKKY interaction that favours a magnetically ordered ground state frequently leads to low-lying phase transitions. External tuning parameters such as magnetic field or pressure can either stabilize or weaken the order. This is usually reflected by an enhancement or a suppression of the ordering temperature. If the ordering temperature can be fully suppressed to zero, a quantum phase transition is accessed. The transition between two distinct ground states may happen in a discontinuous way – by a first order quantum phase transition, or be continuous. In the latter case, we refer to it as quantum critical point (QCP). The interest in these zero-temperature singularities stems from the observation that finite-temperature properties show unconventional behaviour in the vicinity of a QCP.

A theoretical description of quantum critical behaviour was derived by extending the theory of classical criticality to zero temperature.^{3,4} Agreement between experiment and the predicted power laws and scaling relations was found in some cases, but pronounced deviation have also been observed. These latter have led to the development of scenarios where the criticality is not merely due to the vanishing of the order parameter but where another mode is simultaneously critical. A prominent example is the theory of local quantum criticality.⁵ In this theory of the antiferromagnetic (AFM) Kondo lattice with strong two-dimensional spin fluctuations, in addition to the order parameter also the Kondo interaction is suppressed to zero at the QCP. Experimental evidence supporting this “Kondo destruction” scenario has been reviewed recently.^{6,7}

Interestingly, some experiments suggest that both energy scales can also be detached from each other.^{8,9} This can be rationalized in a global phase diagram of AFM heavy fermion quantum criticality.^{10–12} The two parameters that span this zero-temperature phase diagram are the Kondo interaction J_K and the frustration parameter G . It was recently pointed out that G may be identified with spacial dimensionality and, in particular, that cubic compounds are good candidates for probing the global phase diagram in the limit of “high dimensionality” (low G).¹³

Here we thus review cubic heavy fermion compounds for which low-lying phase transitions have been observed. We constrain ourselves to pure (non-substituted) Ce-based heavy

fermion compounds that can be tuned by magnetic field or pressure. We are not aware of any previous review on this topic and hope that it will be a useful guide for future research.

II. ORDERED PHASES

In various cubic Ce-based heavy fermion compounds, low-lying phase transitions have been observed and were shown to depend on non-thermal tuning parameters such as magnetic field or pressure. In some of these, the phase transition temperatures could be fully suppressed to zero (or, more precisely, to a value below the accessible temperature range). These cases are of interest here as quantum critical behaviour might emerge from zero-temperature phase transitions.

In Fig.1 magnetic field–temperature phase diagrams of various cubic Ce-based heavy fermion compounds hosting putative quantum critical points are shown.

A. CeB₆

The oldest and most thoroughly studied among these material is certainly CeB₆. It crystallizes in the cubic CaB₆-type structure of space group $Pm\bar{3}m$. Its magnetic field–temperature phase diagram¹⁴ contains three different phases: a paramagnetic phase (I) at high temperatures, an antiferro-quadrupolar (AFQ) phase (II) at intermediate temperatures, and an antiferromagnetic (AFM) phase (III) at the lowest temperatures (Fig.1 a). Under magnetic field, the AFQ ordering temperature T_Q is enhanced. The nature of the AFM order (phase III or III') depends on the direction along which the magnetic field is applied. The Néel transition $T_N(B)$ is claimed to be of second order.¹⁴ Early evidence for phase II being an AFQ phase was indirect. NMR experiments (in finite magnetic fields) revealed a splitting of the ¹¹B resonance line^{15,16} below T_Q , which is evidence for AFM order. Also neutron diffraction can only detect the AFM order induced by a magnetic field.¹⁴ Direct evidence for the AFQ phase came from resonant X-ray scattering (RXS).¹⁷ This technique was first used for 3d electron systems.¹⁸ In CeB₆, the L_3 edge of the Ce ion is probed. The energy level splitting of the 5d orbital, induced by the Coulomb interaction between the 4f and the 5d orbitals upon orbital ordering, gives rise to the RXS signal. The ordering wavevector was determined to be $(1/2, 1/2, 1/2)$ (in units of $2\pi/a$ where a is the lattice parameter) in this

way.¹⁸ High-field measurements up to 60 T revealed a maximum of $T_Q(B)$ of almost 10 K at about 35 T and a decrease to 8 K at 60 T.¹⁹ A full suppression of T_Q has, however, not been achieved yet. Much work has focussed on the determination of the magnetic structure, both the field-induced one below T_Q and the spontaneous one below T_N .^{14,19–21} Various different ordering wave vectors have been identified. At first sight such a complex magnetic behaviour may be surprising in view of the simple crystallographic structure. However, as will be explained in Sect. III below, it may be attributed to the various active multipoles.

B. CeTe

CeTe is a member of the much investigated family of Ce monochalcogenides (CeS, CeSe, CeTe) which crystallize in the face-centered-cubic NaCl-type structure and have been intensively investigated for several decades. In zero magnetic field and at ambient pressure, CeTe undergoes a second-order²² phase transition at about 2 K to a type-II AFM state, with the ordered moments pointing along the magnetic ordering wavevector $(1/2, 1/2, 1/2)$ (Ce moments are aligned ferromagnetically within (111) magnetic planes but point in opposite directions in adjacent (111) planes).²³ The ordered moment was determined to be between $0.15\mu_B$ and $0.3\mu_B$.^{23,24} The magnetic field–temperature phase diagram at ambient pressure and at two different hydrostatic pressures is shown in Fig. 1 b.²⁵ At ambient pressure, application of a magnetic field along the crystallographic [001] direction stabilizes a new phase (phase II) above 1 T.²⁵ In another investigation, phase II was stabilized above 0.5 T for fields along [001] and [110] and above 3.5 T for fields along [111],²⁶ indicating some sample dependence. Hydrostatic pressure at first stabilizes phase I, seen by the slight enhancement of the Néel temperature to 2.4 K at 0.45 GPa and the strongly enhanced critical field H_c^{I-II} of 4 T at this pressure.²⁵ Further increasing pressure weakens phase I again (and possibly changes its nature, therefore it is referred to as phase I') and stabilizes phase II as the dominating phase at 1.2 GPa.²⁵ The close similarity of the phase diagram of CeTe at 1.2 GPa and the ambient-pressure phase diagram of CeB₆ has led to the suggestion that phase II in pressurized CeTe is also an AFQ ordered phase.²⁵

C. CeAg

The intermetallic compound CeAg, with the CsCl-type cubic crystal structure at room temperature, undergoes two successive phase transitions observed in magnetization,^{27,28} Hall effect,²⁸ magnetic susceptibility,²⁸ electrical resistivity,^{29,30} and specific heat measurements:³¹ a quadrupolar, tentatively ferroquadrupolar (FQ),³¹ transition at $T_Q = 17$ K and a ferromagnetic (FM) transition at $T_C = 5.5$ K.²⁸ From magnetization measurements on CeAg single crystals, which show strong anisotropy and magnetoelastic hysteresis for all but the [001] direction,²⁷ a dome-like profile of $T_Q(B)$ with a maximum of about 9 K at 5 T may be extracted. However, as no temperature–magnetic field phase diagram appears to be published, CeAg is not included in Fig. 1.

D. CeIn₃

CeIn₃ crystallizes in the simple cubic AuCu₃-type structure. At 10.2 K, it orders antiferromagnetically with an ordering wavevector $(1/2, 1/2, 1/2)$ ³² as in CeTe. ¹¹⁵In NQR measurements revealed that the moments point along the $\langle 111 \rangle$ direction.³³ The magnetic order was shown to be fully suppressed by a magnetic field of about 60 T (Fig. 1 c).³⁴ There is no evidence for further ordered phases in the accessed temperature and magnetic field range. Thus, the situation in CeIn₃ appears to be simpler than in CeB₆, CeTe, and CeAg.

E. CeOs₄Sb₁₂

The filled skutterudite compound CeOs₄Sb₁₂ crystallizes in the body-centered cubic structure of space group $Im\bar{3}$.³⁵ The Ce atoms are located at the body centre and corners of the cubic structure. They are surrounded by a cage formed by eight corner-sharing OsSb₆ octahedra. The first indication for a low-temperature phase transition in CeOs₄Sb₁₂ came from specific heat measurements which revealed a λ -type anomaly at 1.1 K. However, as the entropy associated with the anomaly is only 2% of $R \ln 2$ the authors concluded that this phase transition is extrinsic.³⁶ Subsequent investigations of the specific heat under magnetic field confirmed the presence of the phase transition and concluded that it is an intrinsic feature of CeOs₄Sb₁₂.^{37,38} The evolution of the phase transition with magnetic field was also tracked by electrical transport³⁹, NMR/NQR,⁴⁰ and elastic constant measurements.⁴¹ The

magnetic field–temperature phase diagram in Fig. 1 d⁴⁰ is delineated by anomalies in the nuclear spin-lattice relaxation rate $1/T_1$,⁴⁰ the electrical resistivity,³⁹ and the specific heat³⁷ of single crystalline $\text{CeOs}_4\text{Sb}_{12}$. The symbols show an initial increase of the characteristic temperature T_0 with increasing magnetic field, and a suppression of T_0 at higher fields. This is similar to the field dependence of the upper transitions of CeB_6 and pressurized CeTe and might thus be due to quadrupolar order. This is supported by the pronounced softening of the elastic constants C_{11} and C_{44} across T_0 .⁴¹ Evidence for the shaded area denoted AFM comes from neutron diffraction experiments where weak AFM reflections with ordering wavevector $(1,0,0)$ were shown to be suppressed by a magnetic field of 1 T.⁴² Apparently, a signature of $T_N(\mu_0 H)$ is also seen in the electrical resistivity,⁴³ though no original data are published.

F. $\text{Ce}_3\text{Pd}_{20}\text{Ge}_6$

$\text{Ce}_3\text{Pd}_{20}\text{Ge}_6$ is a member of the series $R_3\text{Pd}_{20}\text{Ge}_6$ (R = light rare-earth elements) of inter-metallic compounds crystallizing in an ordered variant of the cubic Cr_{23}C_6 -type structure of space group $Pm\bar{3}m$.⁴⁴ In this structure, the rare-earth atoms occupy two different crystallographic sites ($4a$ site forming a face-centered cubic sublattice and $8c$ site forming a simple cubic sublattice), both with cubic point symmetry (O_h and T_d , respectively). In spite of this structurally more complex situation, the magnetic field–temperature phase diagram of $\text{Ce}_3\text{Pd}_{20}\text{Ge}_6$ (Fig. 1 e) is similar to the ones of CeB_6 and pressurized CeTe . The labelling of the different phases was chosen in analogy with CeB_6 .^{45,46} In zero field, two successive phase transitions at 1.2 and 0.7 K were first revealed by specific heat measurements.⁴⁵ The application of a magnetic field along $[001]$ stabilizes the upper transition but suppresses the lower one.^{45,46} Fields along $[110]$ and $[111]$ lead to more complex phase diagrams, with phase II being split into two different phases.

Powder neutron diffraction in zero magnetic field revealed AFM order with the magnetic ordering wavevector $(0,0,1)$ below the lower transition but could not resolve any magnetic order below the upper transition.⁴⁷ This behaviour is distinct from the one observed in a number of other 3-20-6 compounds ($\text{Nd}_3\text{Pd}_{20}\text{Ge}_6$ and $(\text{Nd}, \text{Tb}, \text{Nd}, \text{Ho})_3\text{Pd}_{20}\text{Si}_6$). Here, below the upper transition the rare earth moments at the $8c$ site order antiferromagnetically with the ordering wavevector $(1,1,1)$. Below the lower transition the moments at the $4a$

site order antiferromagnetically with the ordering wave vector $(0, 0, 1)$.⁴⁸ The absence of the $(1, 1, 1)$ order in $\text{Ce}_3\text{Pd}_{20}\text{Ge}_6$,⁴⁸ together with the absence of a clear signature in the magnetic susceptibility at the upper transition⁴⁹ but the existence of pronounced minima in the elastic constants C_{11} and C_{44} at this temperature⁵⁰ indicate that this order is quadrupolar in nature. The pronounced softening of the elastic constant $(C_{11} - C_{12})/2$ and a sizable spontaneous expansion $\Delta L/L = 1.9 \times 10^{-4}$ along the $[001]$ direction were taken as evidence for FQ order with the order parameter O_2^0 .⁴⁶ In an unpublished diffraction experiment on a $\text{Ce}_3\text{Pd}_{20}\text{Ge}_6$ single crystal with a slightly higher Néel temperature of 0.75 K a very weak magnetic signal with the incommensurate ordering wavevector $(0, 0, 0.94)$ was observed below 0.45 K and suggested to be due to Ce moments at the 8c site.⁴⁷

G. $\text{Ce}_3\text{Pd}_{20}\text{Si}_6$

$\text{Ce}_3\text{Pd}_{20}\text{Si}_6$ shows many similarities with its Ge-based sister compound $\text{Ce}_3\text{Pd}_{20}\text{Ge}_6$, but also pronounced differences. The temperature–magnetic field phase diagram for polycrystals was first determined by specific heat measurements.^{13,51,52} In zero magnetic field, $\text{Ce}_3\text{Pd}_{20}\text{Si}_6$ features two phase transitions at about 0.53 K and 0.33 K.⁵¹ The upper transition is enhanced by a magnetic field to a maximum value of 1.2 K at 8 T.¹³ The lower transition was later tracked in detail by transport measurements and was shown to be completely suppressed by a field of 0.9 T.¹³ For single crystals, the magnetic field–temperature phase diagram was first explored by ultrasound experiments⁵³ and later by magnetization⁵⁴ and specific heat measurements.⁵⁵ Exemplarily the phase diagram for field along $[110]$ is shown in Fig. 1 f.⁵⁴ Overall, it is quite similar to the phase diagram obtained for polycrystalline $\text{Ce}_3\text{Pd}_{20}\text{Si}_6$.¹³ For fields along $[001]$ and $[111]$, however, the upper transition gets sizably modified at fields above 2 T.^{53–55} For fields along $[001]$, phase II splits into two phases (II and II') which are stable up to about 2 T and 4 T, respectively, whereas for fields along $[111]$ phase II is stable up to at least 14 T.⁵³ Interestingly, the lower transition temperature is perfectly isotropic with respect to the direction of the magnetic field.^{54,55} This simple behaviour of phase III is in contrast to the complex structure, with multiple subphases, and the anisotropic field response of phase III in $\text{Ce}_3\text{Pd}_{20}\text{Ge}_6$.⁵⁶

Shortly after the two consecutive phase transitions were revealed by specific heat measurements⁵¹ the temperature-dependent magnetic susceptibility was shown to display

a clear anomaly only at the lower of the two transitions.⁵² In analogy with $\text{Ce}_3\text{Pd}_{20}\text{Ge}_6$ this suggests that the upper transition is quadrupolar in nature. The speculation that quadrupolar effects are involved was further nourished by the observation of a pronounced softening of the elastic constants at low temperatures,⁵⁷ which is typical of $4f$ electrons with a Γ_8 ground state. The temperature and field dependence of the elastic constants were argued to be best described by AFQ order of Γ_8 states at the $8c$ site.⁵³

III. CRYSTAL ELECTRIC FIELD EFFECTS

In cubic symmetry, the crystal electric field (CEF) splits the sixfold degenerate $^2F_{5/2}$ multiplet of the $\text{Ce}^{3+} 4f^1$ state into a Γ_7 doublet and a Γ_8 quartet. The Γ_7 system supports only dipoles but in the Γ_8 system there are various active multipoles: three dipoles, five quadrupoles, and seven octupoles.⁵⁸ Due to the different symmetries of the quadrupolar moments and the dipolar and octupolar moments, quadrupolar ordering cannot induce additional moments in zero magnetic field. However, the application of a field lowers the symmetry and thus quadrupolar order will in general be accompanied by other moments induced by the external field.⁵⁸

In heavy fermion systems, the $\text{Ce}^{3+} 4f^1$ state interacts with conduction electrons (c - f hybridization). This leads to a broadening of the CEF split levels. A strong and anisotropic c - f hybridization might, in addition, even lead to a lowering of the cubic point symmetry and thus to a modification of the theoretically expected level scheme. Thus, the experimental determination of the level scheme in heavy fermion systems is far more challenging than in well localized f electron systems.

Generally, the energy splitting between the ground state and excited levels can be measured by any spectroscopic technique, provided the matrix element for that transition is sufficiently large. Typically, inelastic neutron scattering is employed,^{59–63} but Raman spectroscopy⁵⁹ has also proven useful. If the CEF splitting is small and the broadening due to the c - f hybridization is large, it may be difficult to distinguish the CEF excitation (e.g., inelastic $\Gamma_7 \rightarrow \Gamma_8$ transition) from quasielastic scattering (e.g., elastic $\Gamma_7 \rightarrow \Gamma_7$ scattering).³² To decide which of the levels is the ground state requires a careful determination of the scattering intensities/magnetic form factors and usually further experimental evidence (entropy, magnetization, elastic constants, ...) is used to support the assignment. A rather new tech-

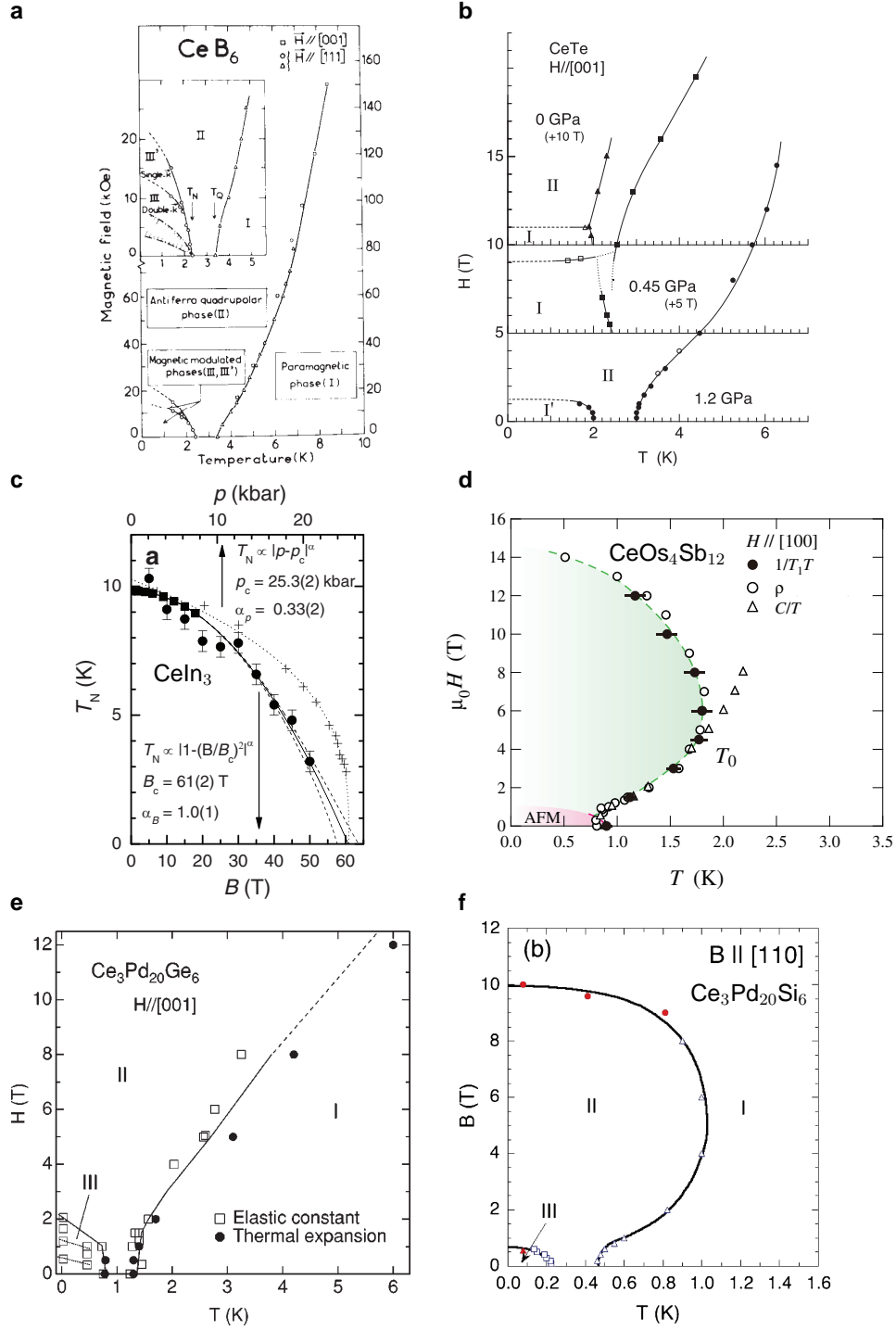


FIG. 1: (Color online) Magnetic field–temperature phase diagrams of (a) CeB₆,¹⁴ (b) CeTe,²⁵ (c) CeIn₃,³⁴ (d) CeOs₄Sb₁₂,⁴⁰ (e) Ce₃Pd₂₀Ge₆,⁴⁶ and (f) Ce₃Pd₂₀Si₆.⁵⁴ In panel c, temperature is plotted on the vertical axis, magnetic field (and pressure, top) on the horizontal axis.

nique that can provide direct evidence for the CEF ground state level is resonant inelastic X-ray scattering.⁶⁴ However, for systems with cubic point symmetry information on the ground state wave function has to date only been extracted in finite magnetic fields.⁶⁵

In CeB_6 , the situation has long been unclear due to conflicting level schemes proposed from various thermal, magnetic and elastic data. Finally, inelastic neutron scattering revealed an energy splitting of 535 K (46 meV). From the temperature-dependent frequency shift of the Raman scattering signal a splitting of 30 K was deduced and taken as evidence for the (weakly split) Γ_8 quartet being the ground state.⁵⁹ This is consistent with the experimentally observed AFQ ordering in zero field and the field-induced magnetic order below $T_Q(B)$.

In CeTe , on the other hand, the Γ_7 doublet was reported to be the ground state and the Γ_8 quartet the excited state at 32 K above.⁶⁰ Unfortunately, both the original neutron scattering data supporting the energy splitting of 32 K as well as the high-field magnetization measurements supporting the Γ_7 ground state appear to be unpublished. Specific heat and magnetic susceptibility failed to give clear indications for the CEF splitting²² but elastic constants measurements were found to be consistent with the splitting of 32 K.⁶⁶ Quadrupolar order cannot directly result from a Γ_7 ground state because it does not have quadrupolar degrees of freedom. However, a mixing of Γ_8 components into the Γ_7 ground state can occur⁶⁷ and has been proposed as mechanism for the pressure induced putative AFQ order of CeTe .²⁵ In fact, fits to the temperature dependence of the magnetization at various pressures yielded a reduction of the CEF splitting with pressure. This was suggested to be responsible for stabilizing the AFQ order under pressure.²⁵ Also the enhancement of the AFQ phase transition temperature under magnetic field is consistent with this scenario.⁶⁷

In CeAg , inelastic neutron scattering experiment observed a CEF excitation at about 265 K (23 meV).⁶⁸ Magnetoelastic measurements assigned the Γ_8 quartet as the CEF ground state.^{27,69}

The CEF level scheme of CeIn_3 was explored by inelastic neutron scattering on powder^{32,70} and single crystalline samples.⁷¹ A broadened CEF excitation is observed at about 140 K (12 meV).^{32,70,71} From an analysis of the magnetic susceptibility the Γ_7 doublet was suggested to be the ground state.⁷² This was later confirmed by magnetic form factor measurements which are best explained with a Γ_7 ground state with some admixture of the Γ_8 wavefunction.⁷³

In $\text{CeOs}_4\text{Sb}_{12}$, the CEF level scheme is still controversial. Inelastic neutron scattering on $\text{CeOs}_4\text{Sb}_{12}$ powder revealed two broad magnetic excitations centered at 315 K (27 meV) and 555 K (48 meV).⁶² One of them might be due to a CEF excitation, broadened by the c - f hybridization, even though an interpretation of these features as indirect and direct transition across a hybridization gap was preferred.⁶² The temperature dependence of the magnetic susceptibility is best described by a level scheme with a Γ_7 ground state separated by 325 K (28 meV) from the Γ_8 excited state.³⁶ The exponential temperature dependence of the NQR relaxation rate $1/T_1$ with an activation energy of 330 K⁷⁴ may be taken as confirmation of this splitting. However, the authors take the lack of a minimum of the elastic constant $(C_{11} - C_{12})/2$,⁴¹ expected for the above level scheme at 0.5×330 K, as evidence against this interpretation and suggest instead that a hybridization gap opens in $\text{CeOs}_4\text{Sb}_{12}$.⁷⁴

Inelastic neutron scattering on $\text{Ce}_3\text{Pd}_{20}\text{Ge}_6$ revealed excitations at 60 K (5.2 meV) and 46 K (4 meV).⁶¹ Since the magnetic entropy reaches $R \ln 4$ per Ce-mole at about 10 K the Γ_8 wave function was assumed to be the ground state.⁴⁹ From the ratio of the intensities of the two excitations the one at 60 K was associated with the $4a$ site and the one at 46 K with the $8c$ site.⁶¹

In inelastic neutron scattering on $\text{Ce}_3\text{Pd}_{20}\text{Si}_6$, on the other hand, only one excitation at 44 K (3.8 meV) was clearly resolved.^{63,75} This could either imply that the excitation energy is similar for both Ce sites and that the peak thus contains both excitations, or that the excitation energy of the second site is much smaller or much larger than 44 K. An analysis with a very low excitation energy of only 3.6 K (0.31 meV) for the $8c$ site was attempted⁶³ but the subtraction of the large quasielastic signal puts large uncertainties on this analysis. The magnetic entropy exceeds $3R \ln 2$ per formula unit already at 1.5 K.⁷⁶ If the excitation energy is 44 K for both Ce sites, this would imply that at least at one of the Ce sites assumes a Γ_8 ground state. Further investigations are needed to clarify the situation.

IV. STRUCTURAL TRANSITIONS

One important question is whether the orbital ordering observed in most of the systems discussed above is associated with a structural transition. This may reduce the cubic symmetry of the system and thus change the degree of frustration (the value of G in the global

phase diagram). In transition metal oxides, orbital order frequently leads to a Jahn-Teller lattice distortion and thus to a lowering of the symmetry.^{77,78} This is due to the large spacial spread of the $3d$ electron orbitals which leads to a strong coupling with the lattice. $4f$ electrons are more localized and thus their coupling with atomic displacements is expected to be weaker.

In CeB_6 a high-resolution neutron powder diffraction investigation has searched for lattice distortions in the vicinity of T_Q and T_N . Within the accuracy of the experiment, which was 0.0003 \AA for the lattice parameter and 0.003° for the angle, no distortion could be detected.²⁰

In CeTe under ambient conditions in magnetic field and pressure, an X-ray diffraction study could not resolve any structural distortion at the transition into phase I. The upper limit for the amplitude of possible distortions was set to 10^{-3} lattice units by this experiment.²³ Only at very high pressures (8 GPa), a structural phase transition from the NaCl-type structure to the CsCl-type structure (both cubic) occurs.⁷⁹

Neutron diffraction experiments on CeAg revealed that the transition at the putative FQ transition T_Q is accompanied by a sizable lattice distortion ($c/a - 1 = 1.9\%$) and thus by a lowering of the symmetry from cubic to tetragonal.⁶⁸

In the temperature–magnetic field phase diagram of CeIn_3 the Néel transition is the only phase transition. Thus, any structural distortion would be expected to accompany this transition. However, neutron diffraction could not reveal any structural change at T_N and the magnetic reflections can be indexed on a doubled unit cell of cubic symmetry.³²

For $\text{CeOs}_4\text{Sb}_{12}$, detailed structural investigations across T_0 are not yet available.

In $\text{Ce}_3\text{Pd}_{20}\text{Ge}_6$, a spontaneous expansion by $\Delta L/L = 1.9 \times 10^{-4}$ along the $[001]$ direction, associated with a transition from cubic to tetragonal symmetry, was observed at the transition between phase I and II. It was taken as evidence for O_2^0 -type FQ ordering.⁴⁶

On $\text{Ce}_3\text{Pd}_{20}\text{Si}_6$, high-resolution neutron diffraction experiments ($\Delta d/d \approx 0.0025$) could not resolve any structural distortion between 40 mK and room temperature.⁶³ The perfectly isotropic behaviour of phase III further supports the absence of a symmetry lowering structural transition.¹³

V. CONTINUOUS VS FIRST ORDER TRANSITIONS

For a finite-temperature phase transition to lead to quantum criticality it needs to remain continuous as it is suppressed down to $T = 0$. A much employed technique to reveal the order of a finite-temperature phase transition is to search for thermal hysteresis effects. The presence of a thermal hysteresis across the phase transition temperature revealed in any of the physical properties is a strong indication for the first order nature of the transition.

Among the compounds discussed above, only for $\text{CeOs}_4\text{Sb}_{12}$ pronounced thermal hysteresis effects were revealed. The temperature dependence of the nuclear spin lattice relaxation rate as well as the full width at half maximum of the NQR spectrum of the Sb nuclei show a hysteresis below T_0 upon heating and cooling the sample.⁷⁴ This indicates that the phase transition at T_0 is of first order.

VI. EFFECT OF PRESSURE

In Sect. II we have discussed the magnetic field–temperature phase diagrams of various cubic Ce-based heavy fermion compounds. Some of these have also been studied under pressure. The purpose of this section is to review these pressure studies and to highlight cases where a pressure-tuned quantum critical point (QCP) has been accessed or may be in reach. In Fig. 2 the temperature–pressure phase diagrams of five different cubic heavy fermion compounds are shown.

For single crystalline CeB_6 , the phase diagram under hydrostatic pressure (Fig. 2 a) was determined by magnetic susceptibility measurements in small fields applied along the [100] direction, using extrapolations to zero field.⁸⁰ The decrease of T_N and the increase of T_Q with pressure were later confirmed by magnetization measurements in larger fields along [110]⁸¹ and [100].⁸² The electrical resistivity $\rho(T)$ of single crystalline CeB_6 was measured under hydrostatic pressure up to 130 kbar.⁸³ A gradual increase of T_Q with pressure is observed up to 50 kbar but at larger pressures the characteristic feature in $\rho(T)$ associated with the transition gets lost. Unfortunately, in this experiment $\rho(T)$ could not detect the transition at T_N . Thus, it is still open whether a pressure-induced QCP can be reached in CeB_6 .

In CeAg , both the putative FQ transition at T_Q and the FM transition at T_C have been studied under pressure. $T_Q(p)$ was tracked by electrical resistivity measurements.

Below 2.2 kbar, T_Q (referred to as T_{M1} by the authors³⁰) is independent of pressure and no thermal hysteresis is observed. At 2.2 kbar and above, T_Q is strongly enhanced up to room temperature at 20 kbar and shows pronounced thermal hysteresis^{30,84}. $T_C(p)$ (Fig. 2 b) was derived from magnetic susceptibility measurements under hydrostatic pressure⁸⁵ and from electrical resistivity measurements under hydrostatic⁸⁴ and quasihydrostatic⁸⁶ pressure. Below 10 kbar, according to all three experiments, T_C increases with pressure. At higher pressures, T_C decreases according to the former two experiments but saturates and then further increases according to the latter experiment. Sample dependencies below T_Q were attributed to different initial strains in the samples due to different growth processes³¹. Such effects might be responsible for these conflicting results. At pressures above 30 kbar no signs of a FM transition were detected down to 2 K.⁸⁵ This might suggest that ferromagnetism is suppressed in a sharp first order transition at pressures slightly above 30 kbar. Clearly, further experiments are needed to clarify the situation.

In CeIn₃, the pressure evolution of the Néel temperature was first determined by electrical resistivity measurements, which show a discontinuity in the temperature gradient at T_N .⁸⁷ Hydrostatic pressure continuously suppresses T_N from 10 K at ambient pressure to below 3 K at 25 kbar. Beyond this pressure, the signature in the electrical resistivity gets lost. A superconducting dome appears in the vicinity of the critical pressure for the full suppression of T_N , estimated to about 26 kbar (Fig. 2 c).⁸⁷ The pressure dependence of T_N ⁸⁸ is plotted together with the field dependence of T_N ³⁴ in Fig. 1 c.

Recently, electrical resistivity under pressure was measured on polycrystalline samples of Ce₃Pd₂₀Ge₆.⁸⁹ At ambient pressure, the temperature dependence of the electrical resistivity shows a clear kink at T_N and a broader feature at T_Q . The evolution of both features with pressure is shown in Fig. 2 d.⁸⁹ Most interesting in the context of quantum criticality is that, at high pressures, both T_N and T_Q decrease. A linear extrapolation of the data above 30 kbar leads to an estimation of the critical pressures $p_{Q,c} = 75$ kbar and $p_{N,c} = 69$ kbar for the full suppression of T_Q and T_N , respectively. Uniaxial pressure investigations on single crystalline Ce₃Pd₂₀Ge₆ up to 3 kbar could not resolve any change of T_Q and T_N , in agreement with the above results. However, sizable changes are seen in finite magnetic fields.⁹⁰

Polycrystalline Ce₃Pd₂₀Si₆ has only very recently been studied under pressure. The evolution of T_N and T_Q with hydrostatic pressure (Fig. 2 e) was determined by electrical resistivity, magnetoresistance and specific heat measurements.⁹¹ T_N increases almost linearly

with pressure whereas T_Q decreases. A linear extrapolation of both dependencies suggests that $T_N(p)$ and $T_Q(p)$ intersect at 7 kbar. Ongoing measurements under higher pressure will reveal whether T_Q and/or T_N can be fully suppressed by pressure.

VII. QUANTUM CRITICAL BEHAVIOUR

In spite of the wealth of information on magnetic field- and pressure-tuned phase transitions in cubic Ce-based heavy fermion compounds presented above, investigations of quantum criticality have been carried out only in few cases.

An interesting early observation on CeB_6 is that the Sommerfeld coefficient γ of the Fermi liquid (FL) contribution to the specific heat, $C = \gamma T$, as well as the A coefficient of the FL form of the electrical resistivity, $\rho = \rho_0 + AT^2$, show cusp-like enhancements near the critical field for the suppression of the AFM phase of about 1.3 T (Fig. 3 a).⁹² Such field dependences are today considered as strong indications for quantum criticality.

CeIn_3 is certainly the most prominent Ce-based quantum critical compound with cubic crystal structure.^{34,87,88,93,94} As discussed above, the Néel transition can be continuously suppressed to zero by either a magnetic field or by pressure. In the vicinity of the critical pressure $p_c = 26.5$ kbar, the temperature dependence of the electrical resistivity shows clear deviations from FL behaviour and is better described by the non-Fermi liquid (NFL) form $\rho = \rho_0 + A_n T^n$ (Fig. 3 b).⁹³

Also in $\text{Ce}_3\text{Pd}_{20}\text{Si}_6$, quantum critical behaviour has been observed,¹³ with the electrical resistivity close to the critical field $\mu_0 H_c = 0.9$ T being best described by a NFL form with an exponent $n = 1$.⁵² The A coefficient of the FL form, determined at the lowest temperatures away from H_c , is strongly enhanced towards H_c (Fig. 3 c).⁹⁵ Isothermal field dependences of the longitudinal and transverse magnetoresistance and the Hall coefficient show a crossover at a characteristic field H^* that coincides with H_c only in the zero-temperature limit.¹³ The width of the crossover sharpens with decreasing temperature in a pure power-law fashion, resulting in a sharp step in the extrapolation to zero temperature, much like the situation in the tetragonal heavy fermion compound YbRh_2Si_2 .^{96,97} This extrapolated zero-temperature discontinuity in the transport properties was interpreted^{13,96,97} as Kondo destruction.^{5,98} In simple terms, at a Kondo destruction QCP the f component of the itinerant electrons localizes and thus drops out of the Fermi sea. This changes the Fermi volume from “large”

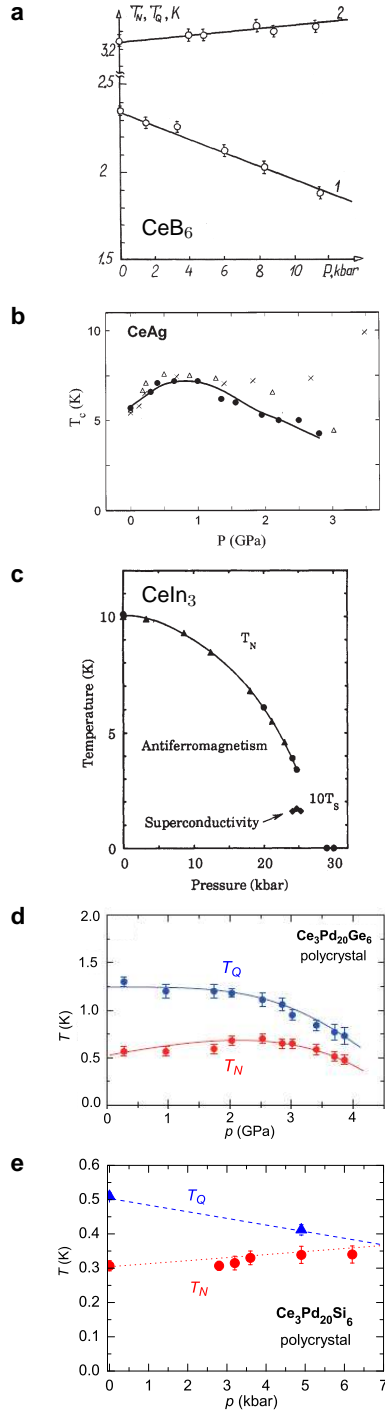


FIG. 2: (Color online) Temperature–pressure phase diagrams of (a) CeB_6 ,⁸⁰ (b) CeAg (\bullet from $\chi(T)$,⁸⁵ \triangle from $\rho(T)$,⁸⁶ and \times from $\rho(T)$ ⁸⁴), (c) CeIn_3 ,⁸⁸ (d) $\text{Ce}_3\text{Pd}_{20}\text{Ge}_6$,⁸⁹ and (e) $\text{Ce}_3\text{Pd}_{20}\text{Si}_6$.⁹¹ T_N , T_C , T_Q , and T_S denote the Néel, Curie, quadrupolar, and superconducting transition temperatures. Measurements were performed on single crystals if not stated otherwise.

to “small”. As a consequence, local moment order may occur. As low-dimensional spin fluctuations are needed in the formulation of the theory,⁵ it was considered unlikely that a Kondo destruction QCP could appear in three-dimensional systems. In cubic $\text{Ce}_3\text{Pd}_{20}\text{Si}_6$, the AFM phase is isotropic^{54,55} and thus it seems plausible to consider it as three-dimensional system. The global phase diagram for AFM heavy fermion compounds^{9–12} provides a way to think about the unexpected Kondo destruction in this compound.¹³ In the region of small values of the magnetic frustration parameter G , a transition from an antiferromagnet with small Fermi surface to an antiferromagnet with large Fermi surface is predicted. In fact, the Kondo destruction QCP in $\text{Ce}_3\text{Pd}_{20}\text{Si}_6$ occurs at the critical magnetic field for the suppression of antiferromagnetism (phase III in Fig. 1 f), inside the putative AFQ ordered phase (phase II in Fig. 1 f). Magnetic fields are likely to induce magnetic dipolar moments on top of the ordered quadrupolar moments.⁹⁹ Thus, it appears plausible that the Kondo destruction QCP in $\text{Ce}_3\text{Pd}_{20}\text{Si}_6$ indeed separates to antiferromagnetic phases.

Interestingly, in CeIn_3 the effective mass of heavy r -orbitals observed in de Haas-van Alphen (dHvA) experiments appears to diverge at a field of about 40 T that is well below the critical field of 61 T for the suppression of antiferromagnetism.⁹⁴ The AFM order is claimed to change its nature from itinerant to local moment at the same field (40 T)⁹⁴ and thus electrical transport signatures of a Kondo destruction would be expected. Unfortunately, the presence of large fields may complicate such analysis¹⁰⁰ and a careful modeling of the background contribution may be needed.

The quantum critical behaviour discussed above occurs at the border of or inside an AFM ordered phase. According to the phase diagrams in Figs. 1 and 2, magnetism is more readily suppressed by magnetic field or pressure than quadrupolar order. To the best of our knowledge, no evidence for quadrupolar quantum criticality has been provided to date in any Ce-based heavy fermion compound. A first indication thereof may be the anomalous field dependence of the A coefficient of the electrical resistivity recently observed on a $\text{Ce}_3\text{Pd}_{20}\text{Si}_6$ single crystal in magnetic fields applied along the [100] direction.¹⁰¹ For this direction quadrupolar order is suppressed already at about 4 T,^{53–55} and it is at this field where the anomaly in $A(H)$ is seen.¹⁰¹

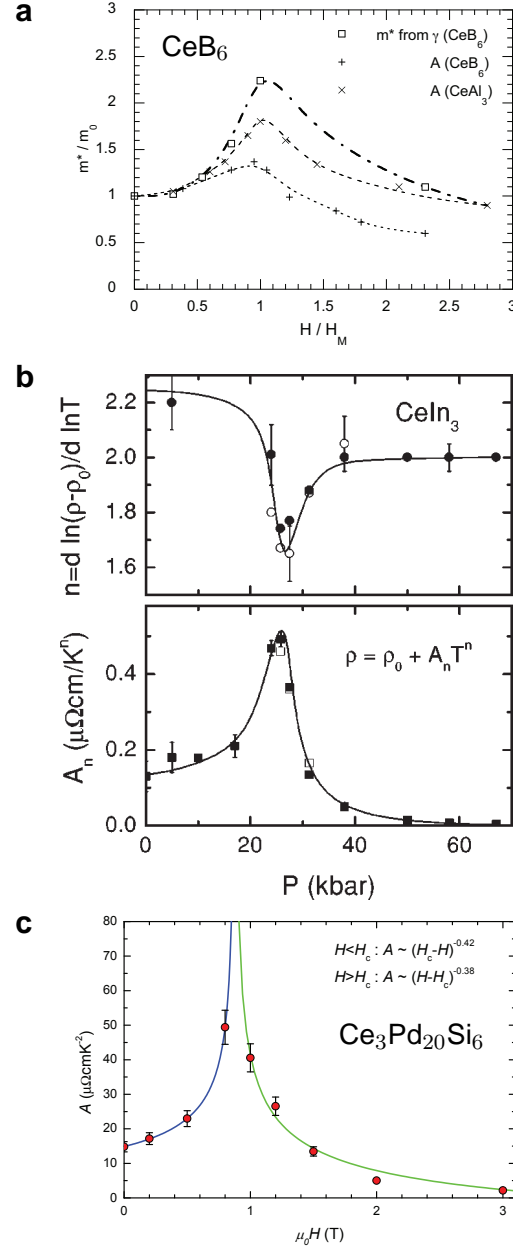


FIG. 3: (Color online) Characteristics of quantum criticality in CeB_6 , CeIn_3 , and $\text{Ce}_3\text{Pd}_{20}\text{Si}_6$. (a) Reduced effective mass deduced from γ and A vs reduced magnetic field ($\mu_0 H_M = 1.3$ T) for CeB_6 ,⁹² (b) resistivity exponent n and generalized resistivity coefficient A_n vs pressure for CeIn_3 ,⁹³ and (c) A vs magnetic field for $\text{Ce}_3\text{Pd}_{20}\text{Si}_6$.⁹⁵ The plot in (a) was remade by C. Marcenat because the corresponding plot in the original reference⁹² is not electronically available is sufficient quality.

VIII. SUMMARY AND OUTLOOK

In this brief review, we have assembled information on Ce-based cubic heavy fermion compounds that show low-lying, tunable phase transitions and are as such candidates to further explore heavy fermion quantum criticality in the three-dimensional limit.

A discriminating characteristic is the crystal field ground state of the Ce^{3+} $J = 5/2$ multiplet. Quadrupolar order appears only if the Γ_8 quartet is the ground state (for at least one crystallographic site) or if there is an important admixture (due to strong c - f hybridization) of the Γ_8 wave function in the ground state. Among the systems reviewed here, CeIn_3 is the only one with a single (antiferromagnetic) phase transition. All others show, in addition to a magnetic transition, a transition attributed to higher multipoles, typically to quadrupoles.

To explore the three-dimensional limit, systems that retain cubic symmetry down to zero temperature are needed. Two of the compounds, CeAg and $\text{Ce}_3\text{Pd}_{20}\text{Ge}_6$, show structural transitions as the quadrupolar order sets in. Interestingly, for both of them, this transition has been identified as ferroquadrupolar. By contrast, at none of the antiferroquadrupolar transitions a structural transition or distortion could be resolved.

Application of a magnetic field to a state with quadrupolar order typically induces magnetic dipolar order on top of the ordered quadrupolar moments. As a consequence, the quadrupolar phase transition temperature acquires field dependence. This is seen for all examples discussed here as an initial enhancement of the quadrupolar ordering temperature with magnetic field. In addition, the field dependence of the quadrupolar ordering temperature is, in general, anisotropic with respect to the direction along which the magnetic field is applied (usually the directions $[001]$, $[110]$, and $[111]$ of the cubic crystal structure are probed). This may, however, not be confused with a breaking of the cubic symmetry of the crystal lattice, which is preserved as long as no symmetry-lowering structural distortion occurs. Pure magnetic dipolar order in cubic systems, on the other hand, is isotropic with respect to the field direction, as experimentally observed for CeIn_3 with a Γ_7 ground state. This distinction may help to identify whether or not the magnetic order in a given material is intimately coupled to quadrupolar order. Details on how the different ordered moments interact with each other and with the conduction electrons remain to be explored.

Finally, we would like to point out that the insulating sister compounds of heavy fermion metals, fully-gapped Kondo insulators, are all cubic. The role of quadrupolar (or higher

multipolar) interactions in Kondo insulators is largely unexplored, and so is the question whether or not these interactions are important for the formation of topological Kondo insulators.¹⁰²

Acknowledgements

We acknowledge fruitful discussions with Q. Si and A. Strydom, and financial support from the European Research Council (ERC Advanced Grant No 227378) and the Austrian Science Fund (FWF project I623-N16). JLJ acknowledges the FRC/URC of the University of Johannesburg for funding of a Postdoctoral Fellowship under joint supervision of SP and A. Strydom. We thank C. Marcenat for providing the plot in Fig. 3 a.

-
- ¹ G. R. Stewart, Rev. Mod. Phys. **73**, 797 (2001).
 - ² H. v. Löhneysen, A. Rosch, M. Vojta, and P. Wölfle, Rev. Mod. Phys. **79**, 1015 (2007).
 - ³ J. Hertz, Phys. Rev. B **14**, 1165 (1976).
 - ⁴ A. J. Millis, Phys. Rev. B **48**, 7183 (1993).
 - ⁵ Q. Si, S. Rabello, K. Ingersent, and J. Smith, Nature **413**, 804 (2001).
 - ⁶ Q. Si and F. Steglich, Science **329**, 1161 (2010).
 - ⁷ Q. Si and S. Paschen, Phys. Status Solidi B **250**, 425 (2013).
 - ⁸ S. Friedemann, T. Westerkamp, M. Brando, N. Oeschler, S. Wirth, P. Gegenwart, C. Krellner, C. Geibel, and F. Steglich, Nature Phys. **5**, 465 (2009).
 - ⁹ J. Custers, P. Gegenwart, C. Geibel, F. Steglich, P. Coleman, and S. Paschen, Phys. Rev. Lett. **104**, 186402 (2010).
 - ¹⁰ Q. Si, Physica B **378-380**, 23 (2006).
 - ¹¹ P. Coleman and A. Nevidomskyy, J. Low Temp. Phys. **161**, 182 (2010).
 - ¹² Q. Si, Phys. Status Solidi B **247**, 476 (2010).
 - ¹³ J. Custers, K. Lorenzer, M. Müller, A. Prokofiev, A. Sidorenko, H. Winkler, A. M. Strydom, Y. Shimura, T. Sakakibara, R. Yu, Q. Si, and S. Paschen, Nature Mater. **11**, 189 (2012).
 - ¹⁴ J. M. Effantin, J. Rossat-Mignod, P. Burlet, H. Bartholin, S. Kunii, and T. Kasuya, J. Magn. Magn. Mater. **47 & 48**, 145 (1985).

- ¹⁵ M. Kawakami, S. Kunii, K. Mizuno, M. Sugita, T. Kasuya, and K. Kume, *J. Phys. Soc. Jpn.* **50**, 432 (1981).
- ¹⁶ M. Takigawa, H. Yasuoka, T. Tanaka, and Y. Ishizawa, *J. Phys. Soc. Jpn.* **52**, 728 (1983).
- ¹⁷ H. Nakao, K. Magishi, Y. Wakabayashi, Y. Murakami, K. Koyama, K. Hirota, Y. Endoh, and S. Kunii, *J. Phys. Soc. Jpn.* **70**, 1857 (2001).
- ¹⁸ Y. Murakami, H. Kawada, H. Kawata, M. Tanaka, T. Arima, Y. Moritomo, and Y. Tokura, *Phys. Rev. Lett.* **80**, 1932 (1998).
- ¹⁹ R. G. Goodrich, D. P. Young, D. Hall, L. Balicas, Z. Fisk, N. Harrison, J. Betts, A. Migliori, F. M. Woodward, and J. W. Lynn, *Phys. Rev. B* **69**, 054415 (2004).
- ²⁰ O. Zaharko, P. Fischer, A. Schenck, S. Kunii, P. Brown, F. Tasset, and T. Hansen, *Phys. Rev. B* **68**, 214401 (2003).
- ²¹ V. P. Plakhty, L. P. Regnault, A. V. Goltsev, S. V. Gavrilov, F. Yakhov, J. Flouquet, C. Vettier, and S. Kunii, *Phys. Rev. B* **71**, 100407 (2005).
- ²² F. Hulliger, B. Natterer, and H. R. Ott, *J. Magn. Magn. Mater.* **8**, 87 (1978).
- ²³ H. R. Ott, J. K. Kjems, and F. Hulliger, *Phys. Rev. Lett.* **42**, 1378 (1979).
- ²⁴ D. Ravot, P. Burlet, J. Rossat-Mignod, and J. L. Tholence, *J. Physique* **41**, 1117 (1980).
- ²⁵ Y. Kawarasaki, T. Matsumura, M. Sera, and A. Ochiai, *J. Phys. Soc. Jpn.* **80**, 023713 (2011).
- ²⁶ M. Nakayama, N. Kimura, H. Aoki, A. Ochiai, C. Terakura, T. Terashima, , and S. Uji, *Phys. Rev. B* **70**, 054421 (2004).
- ²⁷ P. Morin, *J. Magn. Magn. Mater.* **71**, 151 (1988).
- ²⁸ H. Sato, H. Sugawara, Y. Aoki, K. Motoki, R. Settai, and Y. Ōnuki, *J. Phys. Soc. Jpn.* **65**, 1329 (1996).
- ²⁹ H. Ihrig and W. Lohmann, *J. Phys. F: Metal Phys.* **7**, 1957 (1977).
- ³⁰ M. Kurisu, H. Kadomatsu, and H. Fujiwara, *J. Phys. Soc. Jpn.* **52**, 4349 (1983).
- ³¹ P. Morin, J. Rouchy, Y. Miyako, and T. Nishioka, *J. Magn. Magn. Mater.* **76-77**, 319 (1988).
- ³² J. M. Lawrence and S. M. Shapiro, *Phys. Rev. B* **22**, 4379 (1980).
- ³³ Y. Kohori, T. Kohara, Y. Yamato, G. Tomka, and P. C. Riedi, *Physica B* **281-282**, 12 (2000).
- ³⁴ T. Ebihara, N. Harrison, M. Jaime, S. Uji, and J. C. Lashley, *Phys. Rev. Lett.* **93**, 246401 (2004).
- ³⁵ W. Jeitschko and D. J. Braun, *Acta Crystallogr., Sect. B: Struct. Crystallogr. Cryst. Chem.* **33**, 3401 (1977).

- ³⁶ E. D. Bauer, A. Slebarski, E. J. Freeman, C. Sirvent, and M. B. Maple, *J. Phys.: Condens. Matter* **13**, 4495 (2001).
- ³⁷ T. Namiki, Y. Aoki, H. Sugawara, and H. Sato, *Acta Phys. Pol. B* **34**, 1161 (2003).
- ³⁸ C. R. Rotundu and B. Andraka, *Phys. Rev. B* **73**, 144429 (2006).
- ³⁹ H. Sugawara, S. Osaki, M. Kobayashi, T. Namiki, S. R. Saha, Y. Aoki, and H. Sato, *Phys. Rev. B* **71**, 125127 (2005).
- ⁴⁰ M. Yogi, H. Niki, M. Yashima, H. Mukuda, Y. Kitaoka, H. Sugawara, and H. Sato, *J. Phys. Soc. Jpn.* **78**, 053703 (2009).
- ⁴¹ Y. Nakanishi, T. Kumagai, M. Oikawa, T. Tanizawa, M. Yoshizawa, H. Sugawara, and H. Sato, *Phys. Rev. B* **75**, 134411 (2007).
- ⁴² K. Iwasa, S. Itobe, C. Yang, Y. Murakami, M. Kohgi, K. Kuwahara, H. Sugawara, H. Sato, N. Aso, T. Tayama, and T. Sakakibara, *J. Phys. Soc. Jpn.* **77**, 318 (2008).
- ⁴³ H. Sato, Y. Aoki, T. Namiki, T. D. Matsuda, K. Abe, S. Osaki, S. R. Saha, and H. Sugawara, *Physica B* **328**, 34 (2003), proceedings of the Second Hiroshima Workshop on Transport and The rmal Properties of Advanced Materials.
- ⁴⁴ A. V. Gribanov, Y. D. Seropegin, and O. I. Bodak, *J. Alloys Compd.* **204**, L9 (1994).
- ⁴⁵ J. Kitagawa, N. Takeda, M. Ishikawa, T. Yoshida, A. Ishiguro, N. Kimura, and T. Komatsubara, *Phys. Rev. B* **57**, 7450 (1998).
- ⁴⁶ Y. Nemoto, T. Yamaguchi, T. Horino, M. Akatsu, T. Yanagisawa, T. Goto, O. Suzuki, A. Dönni, and T. Komatsubara, *Phys. Rev. B* **68**, 184109 (2003).
- ⁴⁷ A. Dönni, T. Herrmannsdörfer, P. Fischer, L. Keller, F. Fauth, M. A. McEwen, T. Goto, and T. Komatsubara, *J. Phys.: Condens. Matter* **12**, 9441 (2000).
- ⁴⁸ A. Dönni, T. Herrmannsdörfer, P. Fischer, L. Keller, F. Fauth, M. A. McEwen, T. Goto, and T. Komatsubara, *J. Phys.: Condens. Matter* **12**, 9441 (2000, and Refs. herein).
- ⁴⁹ J. Kitagawa, N. Takeda, and M. Ishikawa, *Phys. Rev. B* **53**, 5101 (1996).
- ⁵⁰ O. Suzuki, T. Horino, Y. Nemoto, T. Goto, A. Dönni, T. Komatsubara, and M. Ishikawa, *Physica B* **259-261**, 334 (1999).
- ⁵¹ A. M. Strydom, A. Pikul, F. Steglich, and S. Paschen, *J. Phys.: Conf. Series* **51**, 239 (2006).
- ⁵² S. Paschen, M. Müller, J. Custers, M. Kriegisch, A. Prokofiev, G. Hilscher, W. Steiner, A. Pikul, F. Steglich, and A. M. Strydom, *J. Magn. Magn. Mater.* **316**, 90 (2007).
- ⁵³ T. Goto, T. Watanabe, S. Tsuduku, H. Kobayashi, Y. Nemoto, T. Yanagisawa, M. Akatsu, G.

- Ano, O. Suzuki, N. Takeda, A. Dönni, and H. Kitazawa, *J. Phys. Soc. Jpn.* **78**, 024716 (2009).
- ⁵⁴ H. Mitamura, T. Tayama, T. Sakakibara, S. Tsuduku, G. Ano, I. Ishii, M. Akatsu, Y. Nemoto, T. Goto, A. Kikkawa, and H. Kitazawa, *J. Phys. Soc. Jpn.* **79**, 074712 (2010).
- ⁵⁵ H. Ono, T. Nakano, N. Takeda, G. Ano, M. Akatsu, Y. Nemoto, T. Goto, A. Dönni, and H. Kitazawa, *J. Phys.: Condens. Matter* **25**, 126003 (2013).
- ⁵⁶ T. Sakon, H. Nojiri, A. Ishiguro, N. Tateiwa, A. Sawada, T. Komatsubara, and M. Motokawa, *Physica B* **246-247**, 448 (1998).
- ⁵⁷ T. Watanabe, T. Yamaguchi, Y. Nemoto, T. Goto, N. Takeda, O. Suzuki, and H. Kitazawa, *J. Magn. Magn. Mater.* **310**, 280 (2007).
- ⁵⁸ R. Shiina, H. Shiba, and P. Thalmeier, *J. Phys. Soc. Jpn.* **66**, 1741 (1997).
- ⁵⁹ E. Zirngiebl, B. Hillebrands, S. Blumenröder, G. Güntherodt, M. Loewenhaupt, J. M. Carpenter, K. Winzer, and Z. Fisk, *Phys. Rev. B* **30**, 4052 (1984).
- ⁶⁰ J. Rossat-Mignod, J. M. Effantin, P. Burlet, T. Chattopadhyay, L. P. Regnault, H. Bartholin, C. Vettier, O. Vogt, D. Ravot, and J. C. Achart, *J. Magn. Magn. Mater.* **52**, 111 (1985).
- ⁶¹ L. Keller, A. Dönni, M. Zolliker, and T. Komatsubara, *Physica B* **259-261**, 336 (1999).
- ⁶² D. T. Adroja, J. G. Park, E. A. Goremychkin, K. A. McEwen, N. Takeda, B. D. Rainford, K. S. Knight, J. W. Taylor, J. Park, H. C. Walker, R. Osborn, and P. S. Riseborough, *Phys. Rev. B* **75**, 014418 (2007).
- ⁶³ P. P. Deen, A. M. Strydom, S. Paschen, D. T. Adroja, W. Kockelmann, and S. Rols, *Phys. Rev. B* **81**, 064427 (2010).
- ⁶⁴ T. Willers, Z. Hu, N. Hollmann, P. O. Körner, J. Gegner, T. Burnus, H. Fujiwara, A. Tanaka, D. Schmitz, H. H. Hsieh, H.-J. Lin, C. T. Chen, E. D. Bauer, J. L. Sarrao, E. Goremychkin, M. Koza, L. H. Tjeng, and A. Severing, *Phys. Rev. B* **81**, 195114 (2010).
- ⁶⁵ T. Willers, J. C. Cezar, N. B. Brookes, Z. Hu, F. Strigari, P. Körner, N. Hollmann, D. Schmitz, A. Bianchi, Z. Fisk, A. Tanaka, L. H. Tjeng, and A. Severing, *Phys. Rev. Lett.* **107**, 236402 (2011).
- ⁶⁶ H. Matsui, T. Goto, A. Tamaki, T. Fujimura, T. Suzuki, and T. Kasuya, *J. Magn. Magn. Mater.* **76-77**, 321 (1988).
- ⁶⁷ K. Hanzawa and T. Kasuya, *J. Phys. Soc. Jpn.* **53**, 1809 (1984).
- ⁶⁸ D. Schmitt, P. Morin, and J. Pierre, *J. Magn. Magn. Mater.* **8**, 249 (1978).
- ⁶⁹ R. Takke, N. Dolezal, W. Assmus, and B. Lüthi, *J. Magn. Magn. Mater.* **23**, 247 (1981).

- ⁷⁰ A. P. Murani, A. D. Taylor, R. Osborn, and Z. A. Bowden, Phys. Rev. B **48**, 10606 (1993).
- ⁷¹ W. Knafo, S. Raymond, B. Fåk, G. Lapertot, P. C. Canfield, and J. Flouquet, J. Phys.: Condens. Matter **15**, 3741 (2003).
- ⁷² K. H. J. Buschow, H. W. de Wijn, and A. M. van Diepen, J. Chem. Phys. **50**, 137 (1969).
- ⁷³ J. X. Boucherle, J. Flouquet, Y. Lassailly, J. Palleau, and J. Schweizer, J. Magn. Magn. Mater. **31-34**, 409 (2008).
- ⁷⁴ M. Yogi, H. Kotegawa, G. Zheng, Y. Kitaoka, S. Ohsaki, H. Sugawara, and H. Sato, J. Phys. Soc. Jpn. **74**, 1950 (2005).
- ⁷⁵ S. Paschen, S. Laumann, A. Prokofiev, A. M. Strydom, P. P. Deen, J. R. Stewart, K. Neumaier, A. Goukassov, and J.-M. Mignot, Physica B **403**, 1306 (2008).
- ⁷⁶ N. Takeda, J. Kitagawa, and M. Ishikawa, J. Phys. Soc. Jpn. **64**, 387 (1995).
- ⁷⁷ R. Kajimoto, H. Yoshizawa, H. Kawano, H. Kuwahara, Y. Tokura, K. Ohoyama, and M. Ohashi, Phys. Rev. B **60**, 9506 (1999).
- ⁷⁸ C. D. Ling, J. E. Millburn, J. F. Mitchell, D. N. Argyriou, J. Linton, and H. N. Bordallo, Phys. Rev. B **62**, 15096 (2000).
- ⁷⁹ J. M. Léger, R. Epain, J. Loriers, D. Ravot, and J. Rossat-Mignod, Phys. Rev. B **28**, 7125 (1983).
- ⁸⁰ N. B. Brandt and V. V. Moshchalkov and S. N. Pashkevich and M. G. Vybornov and M. V. Semenov and T. N. Kolobyanina and E. S. Konolova and Yu. B. Paderno, Solid State Commun. **56**, 937 (1985).
- ⁸¹ Y. Uwatoko, M. Kosaka, M. Sera, and S. Kunii, Physica B **281-282**, 555 (2000).
- ⁸² S. Ikeda, M. Sera, S. Hane, Y. Uwatoko, M. Kosaka, and S. Kunii, J. Phys. Soc. Jpn. **76**, 064716 (2007).
- ⁸³ T. C. Kobayashi, K. Hashimoto, S. Eda, K. Shimizu, K. Amaya, and Y. Ōnuki, Physica B **281**, 553 (2000).
- ⁸⁴ H. Fujiwara, M. Kurisu, and H. Kadomatsu, J. Magn. Magn. Mater. **70**, 369 (1987).
- ⁸⁵ A. L. Cornelius, A. K. Gangopadhyay, J. S. Schilling, and W. Assmus, Phys. Rev. B **55**, 14109 (1997).
- ⁸⁶ A. Eiling and J. S. Schilling, Phys. Rev. Lett. **46**, 364 (1981).
- ⁸⁷ I. R. Walker, F. M. Grosche, D. M. Freye, and G. G. Lonzarich, Physica C **282-287**, 303 (1997).

- ⁸⁸ N. Mathur, F. Grosche, S. Julian, I. Walker, D. Freye, R. Haselwimmer, and G. Lonzarich, *Nature* **394**, 39 (1998).
- ⁸⁹ H. Hidaka, S. M. Ramos, E. N. Hering, M. B. Fontes, E. B. Saitovitch, S. Otani, T. Wakabayashi, Y. Shimizu, T. Yanagisawa, and H. Amitsuka, *J. Phys.: Conf. Series* **391**, 012019 (2012).
- ⁹⁰ T. Yamamizu and M. Nakayama and N. Kimura and T. Komatsubara and H. Aoki, *Physica B* **312-313**, 495 (2002).
- ⁹¹ J. Larrea J., A. Strydom, V. Martelli, A. Prokofiev, H. Ronnow, and S. Paschen, to appear in *J. Phys. Soc. Jpn. (Proc. SCES13)*.
- ⁹² C. Marcenat, R. A. Fischer, N. E. Phillips, and J. Flouquet, *J. Magn. Magn. Mater.* **76 & 77**, 115 (1988).
- ⁹³ G. Knebel, D. Braithwaite, P. C. Canfield, G. Lapertot, and J. Flouquet, *Phys. Rev. B* **65**, 024425 (2001).
- ⁹⁴ S. E. Sebastian, N. Harrison, C. D. Batista, S. A. Trugman, V. Fanelli, M. Jaime, T. P. Murphy, E. C. Palm, H. Harima, and T. Ebihara, *PNAS* **106**, 7741 (2009).
- ⁹⁵ K.-A. Lorenzer, Ph.D. thesis, Vienna University of Technology, 2012.
- ⁹⁶ S. Paschen, T. Lühmann, S. Wirth, P. Gegenwart, O. Trovarelli, C. Geibel, F. Steglich, P. Coleman, and Q. Si, *Nature* **432**, 881 (2004).
- ⁹⁷ S. Friedemann, N. Oeschler, S. Wirth, C. Krellner, C. Geibel, F. Steglich, S. Paschen, S. Kirchner, and Q. Si, *PNAS* **107**, 14547 (2010).
- ⁹⁸ P. Coleman, C. Pépin, Q. Si, and R. Ramazashvili, *J. Phys.: Condens. Matter* **13**, R723 (2001).
- ⁹⁹ J. Custers, K. Lorenzer, M. Müller, A. Prokofiev, A. Sidorenko, H. Winkler, A. M. Strydom, Y. Shimura, T. Sakakibara, R. Yu, Q. Si, and S. Paschen, *SI of Nature Mater.* **11**, 189 (2012).
- ¹⁰⁰ S. Bud'ko, V. Zapf, E. Morosan, and P. Canfield, *Phys. Rev. B* **72**, 172413 (2005).
- ¹⁰¹ V. Martelli, J. Larrea J., J. Hänel, K.-A. Lorenzer, A. Prokofiev, and S. Paschen, to appear in *J. Phys. Soc. Jpn. (Proc. SCES13)*.
- ¹⁰² V. Alexandrov, M. Dzero, and P. Coleman, *Phys. Rev. Lett.* **111**, 226403 (2013).